

# Process Tomography of Robust Dynamical Decoupling with Superconducting Qubits

Alexandre M. Souza<sup>1,\*</sup>

<sup>1</sup>Centro Brasileiro de Pesquisas Físicas, Rua Dr. Xavier Sigaud 150, 22290-180, Rio de Janeiro, Brazil

Dynamical decoupling is a technique that protects qubits against noise. The ability to preserve quantum coherence in the presence of noise is essential for the development of quantum devices. Here the Rigetti quantum computing platform was used to test different dynamical decoupling sequences. The performance of the sequences was characterized by Quantum Process Tomography and analyzed using the quantum channels formalism. It is shown that dynamical decoupling can reduce qubit dephasing but cannot protect against spontaneous emission. Furthermore, from process tomography results, it was also possible to conclude that the action of dynamical decoupling cannot be understood as a simple modification of the qubit coherence time. It is also shown here that the performance of dynamical decoupling on the Rigetti's qubits is limited by pulse imperfections. However, the performance can be improved using robust dynamical decoupling, i.e. sequences that are robust against experimental imperfections. The sequences tested here outperformed previous dynamical decoupling sequences tested in the same platform.

## I. INTRODUCTION

In the past decade, there has been a great effort in the development of quantum technologies, such as quantum computers, sensors, and memories. Notable devices are the quantum computers remotely accessible by the public via cloud services. As any quantum system, such computers are subjected to errors arising from unavoidable interactions with the environment or control imperfections. The currently available quantum computers are subjected to a high level of noise. Therefore, these computers are non-fault-tolerant machines, usually referred to as noisy intermediate-scale quantum (NISQ) computers [1]. To make the computation reliable and efficient, it is necessary to use quantum error correction (QEC) codes [2]. The theory of QEC states that it is possible to achieve fault-tolerant quantum computations of arbitrary length provided that the error per gate remains below some threshold [3] and high-fidelity auxiliary states are prepared [4, 5]. However, QEC requires a large number of auxiliary qubits and the practical implementation of QEC codes in the current quantum computers remains a challenge. Therefore, it is desirable to develop methods that can be used to reduce the noise level and control imperfections.

Dynamical decoupling (DD) is a widely used technique to avoid decoherence in quantum systems. The decoupling approach was originally developed in the framework of nuclear magnetic resonance (NMR) [6, 7]. In standard DD, a sequence of  $\pi$ -rotation pulses is periodically applied to a quantum system to attenuate the system-environment interaction. Experimental tests of DD implemented in different types of qubits have demonstrated the increase of the coherence times by several orders of magnitude [8–14]. In nuclear spins in rare-earth-doped crystals, for example, a quantum memory with six-hour coherence

time was achieved by employing decoupling [15]. Apart from preserving the state of a quantum memory, it was also experimentally demonstrated that DD can be used to implement decoherence protected quantum gates [16–20], to enhance the sensitivity of quantum sensors [21, 22] and to characterize the noise spectrum [23–25]. Earlier experiments also showed that the main limitation to DD is pulse imperfections [26].

Using the IBM and Rigetti platforms, it was demonstrated in [27] that DD can protect quantum states of individual qubits and entangled two-qubit states. In that work, it was used the simplest universal decoupling sequence, namely the  $XY-4$ . This sequence is capable to cancel perturbations of the most general environment up to the first order [6], but has little robustness against experimental imperfections [26]. Here we use the Rigetti Computing platform to test different robust DD sequences in superconducting qubits. It is shown that the application of  $XY-4$  can extend the lifetime of a qubit, but also can acts counter productively due to pulse imperfections, while the usage of robust DD can correct the pulse errors. By performing Quantum Process Tomography, it is shown that qubit dephasing is reduced but the ratio in which spontaneous emissions occur cannot be reduced by DD. It is also shown that the action of DD on the qubit dynamics cannot be understood as a simple modification of the qubit coherence time.

This paper is organized as follows. In Sec. II, robust dynamical decoupling sequences are introduced. In Sec. III, the methods used are presented, and in Sec. IV, the results obtained are shown. In the last section, we draw some conclusions.

## II. ROBUST DYNAMICAL DECOUPLING

When a qubit is subjected to an unwanted but static magnetic field, we can preserve the qubit state by refocusing its evolution using a Hahn echo [28], i. e. placing a single rotation by  $\pi$  in the middle of the evolution. If the magnetic field fluctuates in time, the Hahn echo must be

---

\*Electronic address: [amsouza@cbpf.br](mailto:amsouza@cbpf.br)

replaced by DD. The simplest sequence that is capable to refocus magnetic fields fluctuating along the three coordinate axes is the  $XY - 4$ , defined as the repeated application of the basic block  $[\tau/2 - X - \tau - Y - \tau - X - \tau - Y - \tau/2]$ , where  $X$  and  $Y$  are rotations by  $\pi$  about the  $x$  and  $y$  axes and  $\tau$  represents a time during which the qubit evolves freely. Here the coordinate axes are defined as the axes of the qubit Bloch sphere.

The  $XY - 4$  sequence has limited decoupling performance and robustness against experimental imperfections, however, its performance can be improved by different strategies. One strategy is a technique called concatenated dynamical decoupling (CDD) [29–31], where the basic  $XY - 4$  block is concatenated recursively. Another approach was introduced in early NMR experiments [32, 33] and consists of combining one basic building block with a symmetry-related copy. The sequences built within this approach, such as the  $XY - 8$  and  $XY - 16$ , exhibit good robustness against the most common experimental imperfections [26].

It is also possible to build robust DD sequences that do not result from the basic  $XY - 4$ . This is the case of the Knill Dynamical Decoupling (KDD) [34] and the Universally Robust (UR) sequences [35]. The KDD sequence is built from composite pulses, which are sequences of consecutive pulses designed to cancel the most common systematic errors. Therefore, the robustness of the KDD sequence is not achieved due to a form of concatenation. The KDD sequence has been demonstrated to be extremely robust against flip-angle errors and off-resonance errors [34]. The UR sequences are built from a Taylor expansion of the infidelity, which quantifies how far the DD propagator is from a target propagator. The expansion is taken in respect to the imperfect control parameter, while the pulse phases are chosen in order to nullify the series coefficients up to the largest possible order. Considering a DD cycle with  $n$  pulses, where  $n$  is even, it is possible to find a DD sequence robust to flip-angle errors whose  $k$ th pulse phase is given by

$$\phi_k^{(n)} = (k-1)(k-2)\frac{\Phi^{(n)}}{2} + (k-1)\phi_2, \quad (1)$$

$$\Phi^{(n)} = \pm \frac{\pi}{m}, \Phi^{(n)} = \pm \frac{2m\pi}{2m+1}, \quad (2)$$

where  $k = 1 \dots n$  and  $\phi_2$  is an arbitrary phase. When we choose, for example,  $n = 4$  and  $\phi_2 = \pi/2$ , we have  $m = 1$ , in this case the  $XY - 4$  sequence is recovered. High order sequences can be obtained increasing the number of pulses.

e

### III. METHODS

The performance of the sequences must be quantified regardless of the initial state, which is usually not known in most quantum information applications. A good quan-

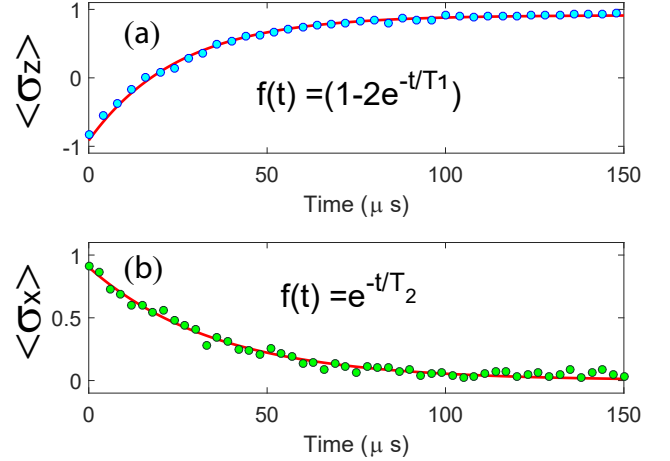


Figure 1: Typical relaxation curves obtained in an inversion recovery experiment (a) and a Hahn echo experiment (b). The experiment were performed in the Rigetti's quantum platform. The relaxation times were determined as  $T_1 = 25\mu s$  and  $T_2 = 35\mu s$ .

tifier for this case is the process fidelity [36]

$$\mathcal{F} = \frac{|\chi_t \chi_{dd}^\dagger|}{\sqrt{\text{Tr}(\chi_t \chi_t^\dagger) \text{Tr}(\chi_{dd} \chi_{dd}^\dagger)}}. \quad (3)$$

Here  $\chi_{dd}$  is the process matrix corresponding to the evolution of the qubit when DD is applied, and  $\chi_t$  is the process matrix corresponding to a target process. The  $\chi$ -matrix can be used to characterize non-unitary dynamics  $\rho_f = \sum_{nm} \chi_{nm} E_n \rho_i E_m^\dagger$ , where  $\rho_i$  and  $\rho_f$  are the density matrices at the beginning and at the end of the evolution. The set of operators  $\{E_m\}$  form a basis. Here we choose the base set as  $\{I, \sigma_x, i\sigma_y \sigma_z\}$ , where  $I$  is the  $2 \times 2$  identity matrix and  $\sigma_k$  is one of the Pauli matrices. Using this basis, the process matrix  $\chi_{dd}$  can be determined by a Quantum Process Tomography [37], while the target matrix,  $\chi_{dd}$ , is given by

$$\chi_t = \begin{bmatrix} 1 & 0 & 0 & 0 \\ 0 & 0 & 0 & 0 \\ 0 & 0 & 0 & 0 \\ 0 & 0 & 0 & 0 \end{bmatrix}. \quad (4)$$

To analyze the qubit dynamics, we can use the quantum channels formalism. The density matrix evolution for a given quantum channel is given by

$$\rho_f = \sum_n K_n \rho_i K_n^\dagger, \quad (5)$$

where  $K_n$  is a Krauss operator [37]. To describe decoherence and relaxation processes of a qubit, it is often used the Amplitude Damping (AD) channel, which describes

the dissipative interactions between the system and its environment, and the Phase Damping (PD) channel, that models the loss of coherence without loss of energy. The Krauss operators corresponding to the simultaneous action of AD and PD can be written as

$$K_1 = \sqrt{\lambda} \begin{bmatrix} 1 & 0 \\ 0 & \sqrt{1-\gamma} \end{bmatrix}, K_2 = \sqrt{1-\lambda} \begin{bmatrix} 0 & \sqrt{\gamma} \\ 0 & 0 \end{bmatrix} \\ K_3 = \sqrt{1-\lambda} \begin{bmatrix} 1 & 0 \\ 0 & \sqrt{1-\gamma} \end{bmatrix}, \text{ and } K_4 = \sqrt{\lambda} \begin{bmatrix} 0 & \sqrt{\gamma} \\ 0 & 0 \end{bmatrix}, \quad (6)$$

where  $\gamma = (1 - e^{\Delta t \beta})$  is the probability that the excited state has decayed to the ground state in the time interval  $\Delta t$  and  $1 - \lambda = (1 - e^{-\Delta t \alpha})/2$  is the probability that the phase  $\phi$ , in the general state  $|\psi\rangle = a|0\rangle + e^{i\phi}b|1\rangle$ , has inverted due to the interaction with the environment. According to this model, the coherence decays exponentially with decay constant  $T_2 = (\alpha + \beta/2)^{-1}$  while all initial states are mapped to the ground state  $|0\rangle$ . For numerical calculations, the evolution of the qubit was discretized into small time steps,  $\Delta t$ , and the equations (5) and (6) were applied recursively.

Usually, when applying DD sequences we aim to remove dephasing. If all dephasing processes were removed ( $\alpha = 0$ ), then we would have  $T_2 = 2T_1$  where  $T_1 = 1/\beta$  is the longitudinal relaxation time. In Figure 1 we can see the results of two experiments performed to measure the relaxation times of a qubit. The transverse relaxation time was measured by a spin echo [28, 38] sequence as  $T_2 = 35\mu s$  and the longitudinal relaxation time was measured by an inversion recovery sequence [38] as  $T_1 = 25\mu s$ . The longest decoherence time,  $T_2$ , achievable for this qubit would be therefore  $50\mu s$ .

#### IV. RESULTS

Using the above formalism, quantum process tomographies of different DD sequences were performed in the Rigetti platform. For each DD tested, a large number of DD cycles were applied to a single qubit in the Aspen-4-2Q-H lattice. After a defined number of cycles, a quantum process tomography was performed and the process fidelity computed to quantify the performance of the sequence.

First, it was studied the performance of the basic  $XY - 4$ . In Figure 2 we see a comparison between the  $XY - 4$  sequence, the Hahn echo, and the free evolution, i.e. when no DD is applied to the qubit. In the case of the free evolution, the fidelity oscillates at the beginning and decay to a constant value. Those oscillations are corrected when the Hahn echo is used, which indicates that a spurious small DC magnetic field might be present. The fidelity is improved by the application of the  $XY - 4$  sequence when the delay between pulses is  $\tau = 120ns$ . However, when the delay is decreased to  $\tau = 80ns$  and  $\tau = 40ns$ , the fidelity drops quickly to a minimum value and then increases until finally stabilizing at a constant value. In an ideal

case, decreasing the delay between pulses should result in better decoupling. However, when errors are present, smaller delays also implies that the error will accumulate faster, resulting in an unwanted effect. The recurrence in the fidelity decay observed for the  $XY - 4$  sequence is similar to those results obtained in NMR experiments [39], where it was found that, in the presence of pulse errors, the  $XY - 4$  sequence can generate an additional effective magnetic field which rotates the qubit. In Figure 3, we can see that the angular frequency,  $\omega$ , increases when  $\tau$  decreases. When robust sequences are used, the oscillation is not observed.

In Figure 2, we can also see that the observed fidelity decay for the Hahn echo is well fitted by the model (6), which combines PD and AD channels. The fitting parameters are  $\alpha = 20.9kHz$  and  $\beta = 23kHz$ . However, the  $XY - 4$  sequence can not be fitted by the same model. In the right panels of the Figure 2, we can see the process matrices obtained at the time instant  $t = 150\mu s$  for the Hahn echo and the  $XY - 4$  sequence. While the process matrix for the Hahn echo is fully compatible with the equations (6), with  $t \rightarrow \infty$ , which map any initial state to the equilibrium state  $|0\rangle$ , the process matrix observed for  $XY - 4$  maps all initial states to a completely depolarized state. This result is interesting and shows that DD does not act merely changing coherence times.

The qubit dynamics can be understood in terms of an effective environment that results from the combination of DD and relaxation processes. When the qubit evolves freely, spontaneous emissions drive the qubit to the ground state. However, a decoupling sequence can take the qubit out from the ground state. The combination of the continuous application of DD pulses with spontaneous emission processes results in the statistical mixture of the ground state and the excited state, as can be seen in the simulations presented in Figure 4. To model this dynamics, we can consider an effective environment which combines phase damping, bit-flip in different directions and unitary rotations. A quantum channel that combines all above features is described by the Krauss operators

$$K_1 = \sqrt{\lambda(1-\gamma)}U, \quad (7)$$

$$K_2 = \sqrt{(1-\lambda)(1-\gamma)}\sigma_z U, \quad (8)$$

$$K_3 = \sqrt{\frac{\gamma}{2}}\sigma_x U, \quad (9)$$

$$K_4 = \sqrt{\frac{\gamma}{2}}\sigma_y U, \quad (10)$$

where  $U = e^{-i\omega\Delta t\sigma_z/2}$ ,  $1 - \lambda = (1 - e^{-\Delta t\alpha})/2$  is the probability of a phase error occur, as in (6), and  $\gamma = (1 - e^{\Delta t\beta})$  is the probability for a bit-flip error occur in  $x$  or  $y$  directions. We can see in Figure 2c that this model fits well the process fidelity for the  $XY - 4$  sequence. The fitting parameters are  $\alpha = 2kHz$ ,  $\beta = 23kHz$ , and  $\omega \approx 10^{-2}rad/ms$  when the delay between pulses is  $\tau = 120ns$ ,  $\alpha = 2kHz$ ,  $\beta = 27kHz$ , and  $\omega = 33rad/ms$  for  $\tau = 80ns$  and  $\alpha = 7kHz$ ,  $\beta = 21kHz$ , and  $\omega = 81rad/ms$

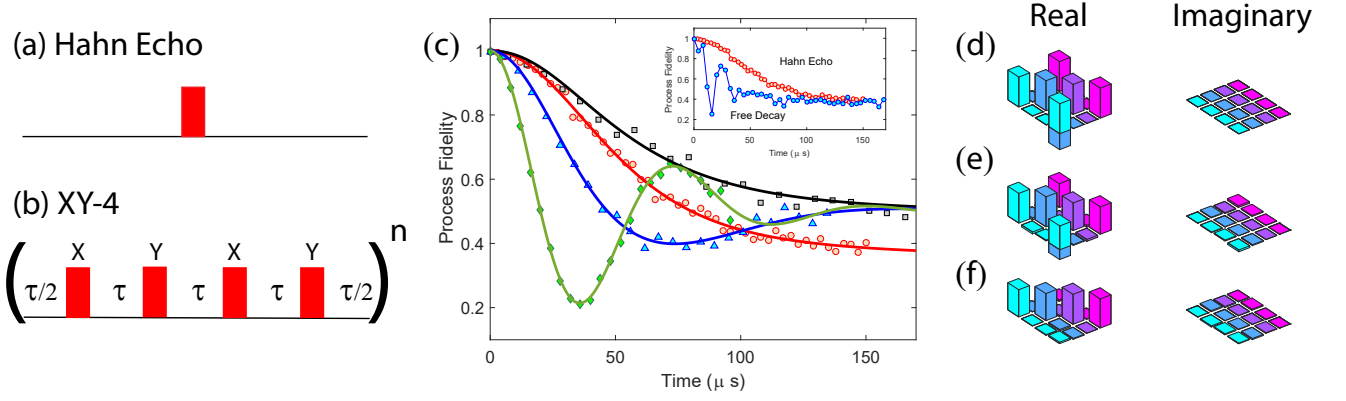


Figure 2: Comparisons between the Hahn echo, the XY-4 sequence, and the free evolution. (a) Illustration of the Hahn echo, a single  $\pi$  pulse, represented by the red rectangle, is placed in the middle of the evolution. (b) Illustration of the XY-4 sequence, the free evolution is replaced by  $n$  applications of the basic XY-4 cycle. (c) Process fidelity as a function of time for the Hahn Echo (red circles) and the XY-4 sequence. The time intervals between the XY-4 pulses are  $\tau = 120 ns$  (black squares),  $\tau = 80 ns$  (blue triangles) and  $\tau = 40 ns$  (green diamonds). The solid lines are the fitted models (see text). The inset shows a comparison between the Hahn Echo and the free evolution of the qubit. (d) The theoretical process matrix representing the quantum channel described by the equations 6, when the evolution time  $t \rightarrow \infty$ . In (e) and (f) we can see the process matrices observed at  $t = 150 \mu s$  for the Hahn echo and the XY-4 sequence, respectively.

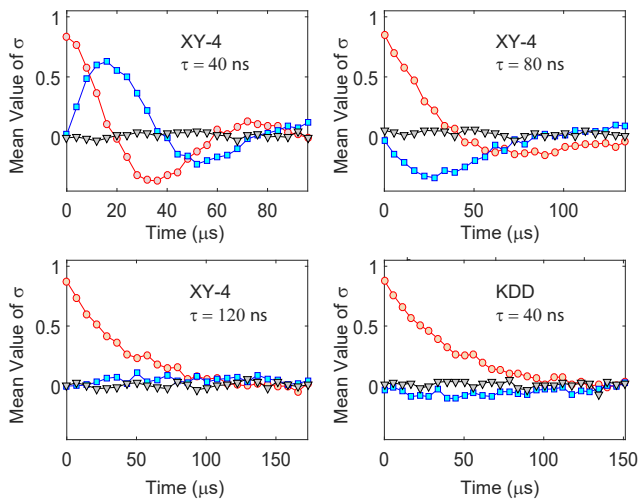


Figure 3: Mean value of the operators  $\sigma_x$  (red circles),  $\sigma_y$  (blue rectangles) and  $\sigma_z$  (black triangles) as a function of time. The initial state is  $(|0\rangle + |1\rangle)/\sqrt{2}$ .

for  $\tau = 40 ns$ .

In Figure 5, we can see the comparison between different DD sequences. The performance of all robust sequences is better than the XY-4 sequence, which has the worst performance among the sequences tested due to the accumulation of errors. The oscillation of the fidelity observed for the XY-4 sequence can be associated with experimental imperfections [39], which causes the qubit to rotate around the  $z$ -axis. All robust sequences eliminates the oscillations. The  $\alpha$  parameter relates to the rate that a phase error occurs; all DD sequences reduce this param-

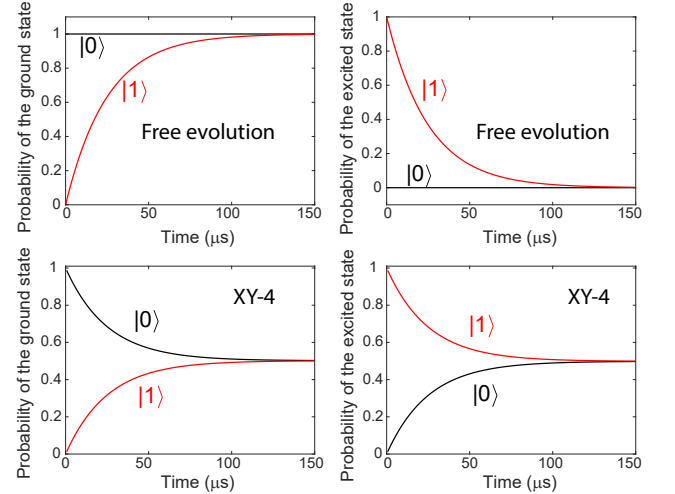


Figure 4: Simulation of the quantum channel described by the equations (6). The simulation starts in the ground state (black curves),  $|0\rangle$ , and the excited state (red curves),  $|1\rangle$ .

eter roughly by a factor of ten when compared to the Hahn echo ( $\alpha = 20.9 kHz$ ). This is a clear indication that DD sequences are mitigating dephasing mechanisms. However, the  $\beta$  parameter, which is related to spontaneous emission, could not be reduced. Furthermore, the combination of robust DD and spontaneous emission also results in an effective environment that maps all states to a completely mixed state. All curves in the Figure 5 were fitted with the same effective channel described above. When we observe the survival probability of the excited state as a function of time (see Figure 6), we can see that

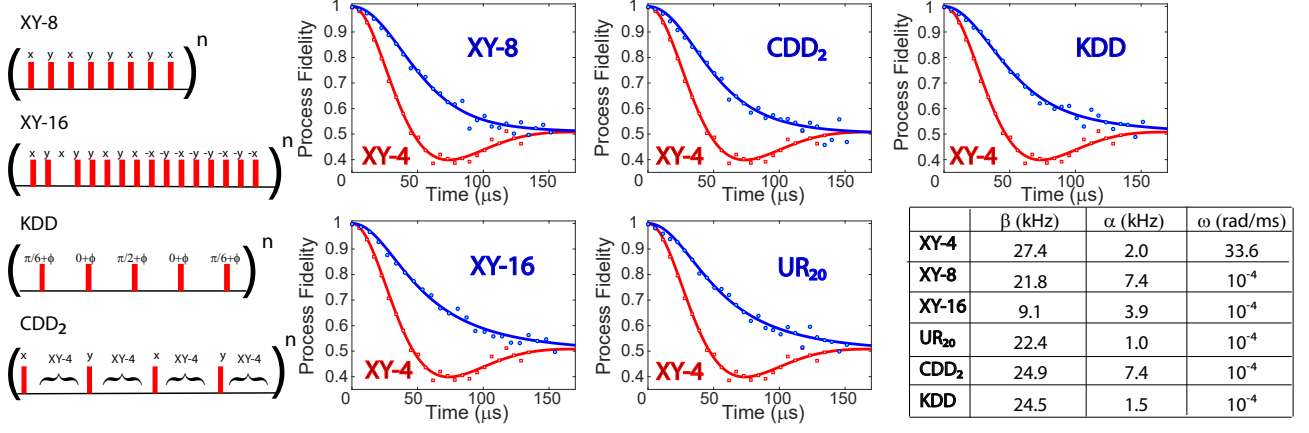


Figure 5: Fidelity process as a function of time for different robust sequences, as indicated in each panel. The left panel illustrates the DD sequences tested, the delay between pulses is kept fixed as  $\tau = 80ns$  in all cases. The phase  $\phi$  in the KDD sequence alternates between two values: 0 and  $\pi/2$ . The basic cycle of the UR20 sequence, not shown, is composed by 20 pulses with phases given by  $\phi_k = (k-1)(k-2)\pi/10 + (k-1)\pi/2$  where  $k = 1 \dots 20$  [35]. The table shows the fitting parameters for each sequence.

DD sequences appear to protect the state against spontaneous emission, as noted in [27]. However, the apparent better performance of DD here is due to the fact that DD randomize the qubit state, the ratio in which the spontaneous emission occurs, as quantified by  $\beta$ , does not change significantly. Still, from Figures 2 and 5 we can conclude that the usage of robust DD is preferable than non-robust sequences.

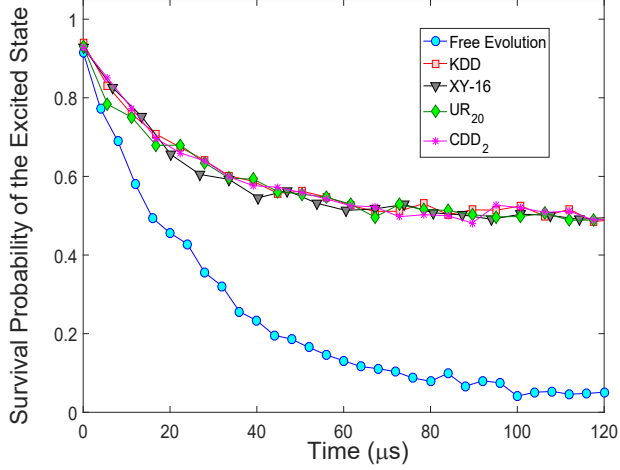


Figure 6: Survival Probability of the excited state  $|1\rangle$  as a function of time.

## V. CONCLUSION

The ability to preserve quantum coherence in the presence of noise is essential to the development of quantum

devices. Dynamical decoupling is a widely used technique to protect qubits against noise. Early experiments have demonstrated the usefulness of DD in many different types of qubits. Here, different DD sequences were tested in a cloud-based quantum computer. The performance of the sequences were characterized by Quantum Process Tomographies. While decoherence and relaxation processes without DD are well modeled by a combined action of amplitude damping and phase damping channels, the application of DD results in different dynamics, which can be viewed as an effective new environment. As in early experimental tests of DD, it was also shown here that the effect of pulse imperfections can lower the sequence performance. Therefore the usage of robust DD sequences, designed to mitigate experimental errors, are preferred over non-robust sequences. The results reported here help in understanding the dynamics of superconducting qubits when DD is applied and demonstrate the usefulness of DD on the current available noisy quantum computers. In the future it is expected that DD could be combined with error correction codes [40, 41] to improve the fidelity of quantum gates. Another attractive prospect for future work is the implementation of DD in other platforms, such as the quantum computers based on trapped ions technology.

## Acknowledgments

This work was supported by the Brazilian National Institute of Science and Technology for Quantum Information (INCT-IQ) Grant No. 465469/2014-0, the National Council for Scientific and Technological Development (CNPq) and FAPERJ (Grant No. 203.166/2017). The author also acknowledges Rigetti Computing for giv-



ing access to the quantum computing platform.

- 
- [1] J. Preskill, Quantum **2**, 79 (2018), URL <https://doi.org/10.22331/q-2018-08-06-79>.
  - [2] E. Campbell, B. Terhal, and C. Vuillot, Nature **549**, 172 (2017).
  - [3] E. Knill, R. Laflamme, and W. Zurek, Science **279**, 342 (1998).
  - [4] S. Bravyi and A. Kitaev, Phys. Rev. A **71**, 022316 (2005).
  - [5] A. M. Souza, J. Zhang, C. A. Ryan, and R. Laflamme, Nat. Comm. **2**, 169 (2010).
  - [6] L. Viola, E. Knill, and S. Lloyd, Phys. Rev. Lett. **82**, 2417 (1999).
  - [7] A. G. Álvarez and D. Suter, Rev. Mod. Phys. **88**, 041001 (2016), URL <http://doi.org/10.1103/RevModPhys.88.041001>.
  - [8] M. J. Biercuk, H. Uys, A. P. VanDevender, N. Shiga, W. M. Itano, and J. J. Bollinger, Nature **458**, 1265 (2009).
  - [9] J. Du, X. Rong, N. Zhao, Y. Wang, J. Yang, and R. B. Liu, Nature **461**, 996 (2009).
  - [10] G. deLange, Z. H. Wang, D. Riste, V. V. Dobrovitski, and R. Hanson, Science **330**, 60 (2010).
  - [11] C. A. Ryan, J. S. Hodges, and D. G. Cory, Phys. Rev. Lett. **105**, 200402 (2010).
  - [12] Y. Sagi, I. Almog, and N. Davidson, Phys. Rev. Lett. **105**, 053201 (2010).
  - [13] K. Saeedi, S. Simmons, J. Z. Salvail, P. Dluhy, H. Riemann, N. V. Abrosimov, P. Becker, H.-J. P. adn J. J. L. Morton, and M. L. W. Thewalt, Science **342**, 830 (2013).
  - [14] S. Damodarakurup, M. Lucamarini, G. DiGiuseppe, D. Vitali, and P. Tombesi, Phys. Rev. Lett. **103**, 040502 (2009).
  - [15] M. Zhong, M. P. Hedges, R. L. Ahlefeldt, J. G. Bartholomew, S. E. Beavan, S. M. Wittig, J. J. Longdell, and M. J. Sellars, Nature **517**, 177 (2015).
  - [16] T. van der Sar, Z. H. Wang, M. S. Blok, H. Bernien, T. H. Taminiau, D. M. Toyli, D. A. Lidar, D. D. Awschalom, R. Hanson, and V. V. Dobrovitski, Nature **484**, 82 (2012).
  - [17] X. Rong, J. Geng, Z. Wang, Q. Zhang, C. Ju, F. Shi, C.-K. Duan, and J. Du, Phys. Rev. Lett. **112**, 050503 (2014).
  - [18] J. Zhang, A. M. Souza, F. D. B. ao, and D. Suter, Phys. Rev. Lett. **112**, 050502 (2014), URL <https://link.aps.org/doi/10.1103/PhysRevLett.112.050502>.
  - [19] A. Souza, R. Sarthor, I. Oliveira, and D. Suter, Phys. Rev. A **92**, 062332 (2015), URL <https://link.aps.org/doi/10.1103/PhysRevA.92.062332>.
  - [20] A. M. Souza, G. A. Alvarez, and D. Suter, Phys. Rev. A **86**, 050301(R) (2012).
  - [21] J. M. Taylor, P. Cappellaro, L. Childress, L. Jiang, D. Budker, P. R. Hemmer, A. Yacoby, R. Walsworth, and M. D. Lukin, Nat. Phys. **4**, 810 (2008).
  - [22] A. Cooper, E. Magesan, H. Yum, and P. Cappellaro, Nat. Comm. **5**, 3141 (2014).
  - [23] J. Bylander, S. Gustavsson, F. Yan, F. Yoshihara, K. Harrabi, G. Fitch, D. G. Cory, Y. Nakamura, J.-S. Tsai, and W. D. Oliver, Nat. Phys. **7**, 565 (2011).
  - [24] G. A. Alvarez and D. Suter, Phys. Rev. Lett. **107**, 230501 (2011).
  - [25] Y. Sung, F. Beaudoin, L. M. Norris, F. Yan, D. K. Kim, J. Y. Qiu, U. von Lupke, J. L. Yoder, T. P. Orlando, S. Gustavsson, et al., Nature communications **10**, 1 (2019).
  - [26] A. M. Souza, G. A. Alvarez, and D. Suter, Phil. Trans. R. Soc. A **4748**, 370 (2012).
  - [27] B. Pokharel, N. Anand, B. Fortman, and D. A. Lidar, Phys. Rev. Lett. **121**, 220502 (2018), URL <https://doi.org/10.1103/PhysRevLett.121.220502>.
  - [28] E. L. Hahn, Phys. Rev. **80**, 580 (1950).
  - [29] K. Khodjasteh and D. A. Lidar, Phys. Rev. Lett. **95**, 180501 (2005).
  - [30] G. A. Alvarez, A. Ajoy, X. Peng, and D. Suter, Phys. Rev. A **82**, 042306 (2010).
  - [31] G. A. Alvarez, A. M. Souza, and D. Suter, Phys. Rev. A **85**, 052324 (2012).
  - [32] A. A. Maudsley, J. Magn. Reson. **69**, 488 (1986).
  - [33] T. Gullion, D. B. Baker, and M. S. Conradi, J. Magn. Reson. **89**, 479 (1990).
  - [34] A. M. Souza, G. A. Alvarez, and D. Suter, Phys. Rev. Lett. **106**, 240501 (2011).
  - [35] G. T. Genov, D. Schraft, N. V. Vitanov, and T. Halfmann, Phys. Rev. Lett. **118**, 133203 (2017).
  - [36] X. Wang, C.-S. Yu, and X. Yi, Phys. Lett. A **373**, 58 (2008).
  - [37] M. A. Nielsen and I. L. Chuang, *Quantum computation and quantum information* (Cambridge University Press, 2001).
  - [38] A. Abragam, *Principles of Nuclear Magnetism* (Oxford University Press, 1990).
  - [39] A. M. Souza, G. A. Alvarez, and D. Suter, Phys. Rev. A **85**, 032306 (2012).
  - [40] G. A. Paz-Silva and D. Lidar, Sci. Rep. **3**, 1530 (2013).
  - [41] H. K. Ng, D. A. Lidar, and J. Preskill, Phys. Rev. A **84**, 012305 (2011).